SANDIA REPORT

SAND2005-4868
Unlimited Release
Printed August 2005

A Reduced Order Model for the Study of Asymmetries in Linear Gas Chromatography for Homogeneous Tubular Columns

Michael L. Parks, Louis A. Romero, and Joshua Whiting

Prepared by
Sandia National Laboratories
Albuquerque, New Mexico 87185 and Livermore, California 94550

Sandia is a multiprogram laboratory operated by Sandia Corporation,
a Lockheed Martin Company, for the United States Department of Energy's
National Nuclear Security Administration under Contract DE-AC04-94-AL85000.

Issued by Sandia National Laboratories, operated for the United States Department of Energy by Sandia Corporation.

Available to DOE and DOE contractors from
U.S. Department of Energy
Office of Scientific and Technical Information
P.O. Box 62
Oak Ridge, TN 37831

Telephone: (865) 576-8401
Facsimile: (865) 576-5728
E-Mail: reports@adonis.osti.gov
Online ordering: http://www.doe.gov/bridge

Available to the public from
U.S. Department of Commerce
National Technical Information Service
5285 Port Royal Rd
Springfield, VA 22161

Telephone: (800) 553-6847
Facsimile: (703) 605-6900
E-Mail: orders@ntis.fedworld.gov
Online ordering: http://www.ntis.gov/ordering.htm

SAND2005-4868
Unlimited Release
Printed August 2005

A Reduced Order Model for the Study of Asymmetries in Linear Gas Chromatography for Homogeneous Tubular Columns

Michael L. Parks and Louis A. Romero
Computational Mathematics and Algorithms Department

Joshua Whiting
Micro Analytical Systems Department

Sandia National Laboratories
P.O. Box 5800
Albuquerque, NM 87185-1110

Abstract

In gas chromatography, a chemical sample separates into its constituent components as it travels along a long thin column. As the component chemicals exit the column they are detected and identified, allowing the chemical makeup of the sample to be determined. For correct identification of the component chemicals, the distribution of the concentration of each chemical along the length of the column must be nearly symmetric. The prediction and control of asymmetries in gas chromatography has been an active research area since the advent of the technique. In this paper, we develop from first principles a general model for isothermal linear chromatography. We use this model to develop closed-form expressions for terms related to the first, second, and third moments of the distribution of the concentration, which determines the velocity, diffusion rate, and asymmetry of the distribution. We show that for all practical experimental situations, only fronting peaks are predicted by this model, suggesting that a nonlinear chromatography model is required to predict tailing peaks. For situations where asymmetries arise, we analyze the rate at which the concentration distribution returns to a normal distribution. Numerical examples are also provided.

Acknowledgments

The authors wish to acknowledge many helpful discussions with Robert Simonson of the Micro Analytical Systems department. The authors would also like to acknowledge the support of the CSRF program.

Contents

Figures

Tables

A Reduced Order Model for the Study of Asymmetries in Linear Gas Chromatography for Homogeneous Tubular Columns

1 Introduction

Chromatography [6, 7] is a family of analytical chemistry techniques for the separation of mixtures. Common to all chromatographic techniques is the passing of a sample (the *analyte*) in the *mobile phase* past a static retentative medium called the *stationary phase*. The stationary phase provides resistance to transport via chemical interactions with the components of the sample. Each component in the sample has a characteristic separation rate that can be used to identify it, and thus the composition of the original mixture.

Marcel Golay's paper [5] is one of the most celebrated papers in the field of gas chromatography. While attempting to analyze packed-column chromatography, Golay conceived of using capillary columns rather than packed columns, increasing the separating power by orders of magnitude. In capillary chromatography, the stationary phase is a liquid coating the column walls, and is chosen specifically to interact with the analyte. The mobile phase is an inert carrier gas, frequently hydrogen or helium, that transports the analyte along the column. Different chemicals pass at different rates, allowing separation. An analyte diffuses as it moves down the column, such that the concentration along the long axis eventually assumes the shape of a gaussian. In this paper we revisit the work of Golay, starting from first principles, and provide formal justification for his results, as well as extending them.

For various reasons, the concentration may not assume a symmetric form, making accurate identification of compounds difficult to impossible. For example, high gas flow rates and shorter column lengths will provide a desirable decrease in the analysis time, but can also lead to asymmetric forms. In particular, columns with an inhomogeneous stationary phase are known to produce asymmetric forms [9]. For the case of isothermal linear chromatography in homogeneous columns, we develop a mathematical and computational model describing the movement of an analyte along the column, and determine the concentration shape. We outline the combinations of problem parameters leading to asymmetries, and determine the rate at which an asymmetric concentration distribution returns to normality.

In his fundamental paper, Golay develops a mathematical model for capillary chromatography by extending the work of Taylor [10, 11] and Aris [2] to the case of reacting side walls. Taylor, and later Aris, analyzed the dispersion of a solute flowing through narrow channels. Golay analyzes the diffusion of a sample gas of uniform composition within a round column uniformly coated with a retentive layer. The cross-section of such a column is shown in Figure 1. Golay makes the assumption that diffusion in the stationary phase is instantaneous. Analogously, this implies that the stationary phase is of negligible thickness compared to the column diameter. Using a cylindrical coordinate system with $u_0(r)$ as the

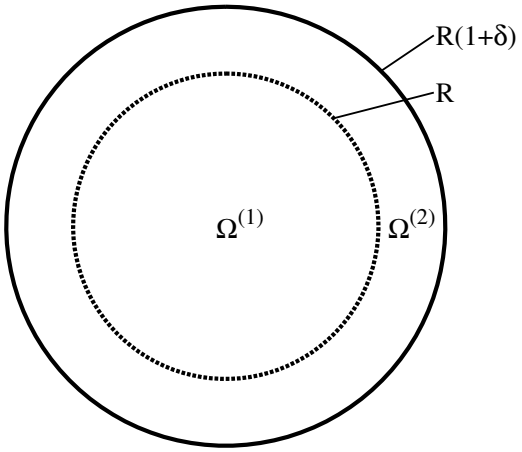

Figure 1. Cross section of a gas chromatography column. $\Omega^{(1)}$ represents the mobile phase, where the analyte is conveyed along the column by a carrier gas. $\Omega^{(2)}$ represents the stationary phase, generally a viscous liquid that interacts with the analyte. Each chemical progresses at a different rate along the column based on how strongly it interacts with the stationary phase. As a result, the chemicals become spatially separated from each other, and exit the column at different times.

expression for Poiseuille flow in a column, Golay considers the equations

$$\frac{\partial C^{(1)}}{\partial t} + u_0\left(r\right)\frac{\partial C^{(1)}}{\partial z} = D^{(1)}\left(\frac{\partial^2 C^{(1)}}{\partial r^2} + \frac{1}{r}\frac{\partial C^{(1)}}{\partial r} + \frac{\partial^2 C^{(1)}}{\partial z^2}\right) \qquad \text{in } \Omega, \tag{1.1}$$

$$\frac{D^{(1)}}{R}\frac{\partial C^{(1)}}{\partial r} = -\frac{k}{2}\frac{\partial C^{(1)}}{\partial t} \qquad \text{at } r = R, \tag{1.2}$$

where $C^{(1)}$ is the concentration in the mobile phase, $D^{(1)}$ is the diffusivity in the mobile phase, R is the capillary radius, and k is the retention factor, defined as the ratio of the analyte in the stationary phase to the analyte in the mobile phase, when there is equilibrium between the two phases. We refer to (1.1) and (1.2) as the *one-domain* model, because only the mobile phase is explicitly modeled, and the stationary phase is reduced to a reactive boundary condition. The first equation in the one-domain model governs the diffusion of the analyte in the column. The second is a reacting-wall boundary condition describing the interaction of the analyte with the stationary phase. The authors know of no derivation for the boundary condition (1.2). Furthermore, it is unclear how this boundary condition should be modified to account for a thicker stationary phase, or to a situation where the thickness of the stationary phase is not much smaller than its radius of curvature, such as the example cross-section in Figure 2. We will address such a case in a future work.

When performing a numerical simulation of chromatography, a boundary condition similar to (1.2) is generally used. However, such simulations are not accurate unless this boundary condition is correct. We set forth the full equations governing gas chromatography in

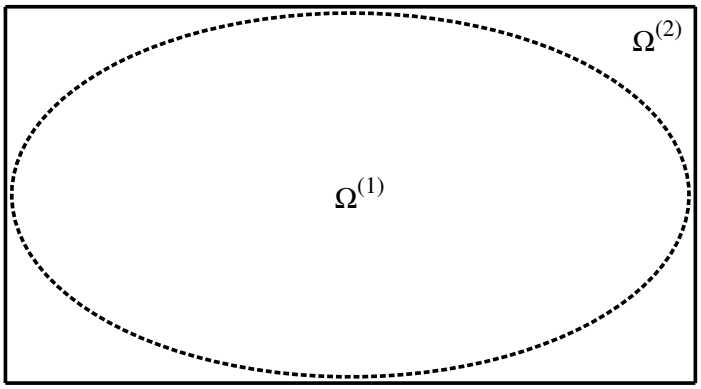

Figure 2. Cross section of gas chromatography column. $\Omega^{(1)}$ represents the region containing the mobile phase and $\Omega^{(2)}$ the region containing the stationary phase. In this figure, the liquid stationary phase has accumulated in the corners, resulting in an undesirably thick coating.

section 2, where we model both the mobile and stationary phases explicitly. No assumptions are made regarding the thickness of the stationary phase or the rate of diffusion in that phase. In section 3.2 we derive the boundary condition (1.2) by performing an asymptotic expansion under the assumption that the stationary phase is thin. For a thicker stationary phase, Golay's boundary condition (1.2) may not give solutions with the desired accuracy.

A direct numerical simulation of a chromatograph is an expensive endeavor, due to the very high aspect ratio of the capillary column. The ratio of the column length to the column diameter can be on the order of 10^5 or more. A brute force numerical simulation requires we explicitly model the entire length of the column, even though very little activity occurs far from the concentration peak. A straightforward computational implementation necessarily leads to poor resource utilization. We instead take a more efficient approach by first performing a Fourier transform along the long axis of the column, effectively removing the undesirable aspect ratio. In section 3, we show that the equations describing gas chromatography in both mobile and stationary phases can be solved by performing a Fourier transform along the long axis and expanding the solution in eigenfunctions $\widehat{C}_m^{(1)}$ and $\widehat{C}_m^{(2)}$ with eigenvalue $\lambda_m(\alpha)$, where m indicates the mode and α the wavenumber. We show that the motion in the column is controlled by the $m = 0$ modes $\widehat{C}_0^{(1)}$ and $\widehat{C}_0^{(2)}$, and the eigenvalue $\lambda_0(\alpha)$, for small α. In section 4, we let σ be the dimensionless rescaling of λ_0, ε be the dimensionless rescaling of α, and consider the expansion

$$\sigma(\varepsilon) = \sigma_0 + i\sigma_1\varepsilon + \sigma_2\varepsilon^2 + i\sigma_3\varepsilon^3 + \dots \tag{1.3}$$

of $\sigma(\varepsilon)$. We show that σ_1 controls the velocity of the analyte in the column, σ_2 controls the diffusion, and that σ_3 controls asymmetry. In sections 4.1 and 4.2 we perform a perturbation expansion of σ_1, σ_2, and σ_3 to construct analytic expressions for these terms, which illustrate the combinations of problem parameters $D^{(1)}$, $D^{(2)}$, k, etc., that will generate asymmetric concentration distributions. This analysis provides a rigorous mathematical explanation of phenomena empirically well understood by gas chromatographers. Further,

we show in section 5 that as the time t becomes large, the effect of σ_3 is diminished, and the concentration resumes a normal distribution. We also address the time necessary for other sources of asymmetry, such as the initial concentration, to dissipate. The optimum carrier gas flow rate and minimum theoretical plate height are computed in section 6. We verify our asymptotic results through numerical experiment in section 7 and offer conclusions in section 8.

2 Fundamental Equations for Linear Gas Chromatography

We begin by writing down the full equations for linear gas chromatography for a general coordinate system and arbitrary column cross-section. Let $\Omega^{(1)}$ denote the mobile phase, and $\Omega^{(2)}$ the stationary phase. We refer to equations (2.1)-(2.5) as the the *two-domain* model. The operative equations are

$$\frac{\partial C^{(1)}}{\partial t} + u_0(x,y)\frac{\partial C^{(1)}}{\partial z} = D^{(1)}\nabla^2 C^{(1)} \qquad \text{in } \Omega^{(1)}, \tag{2.1}$$

$$\frac{\partial C^{(2)}}{\partial t} = D^{(2)}\nabla^2 C^{(2)} \qquad \text{in } \Omega^{(2)}, \tag{2.2}$$

$$C^{(2)} = KC^{(1)} \qquad \text{on } \partial\Omega^{(1)}, \tag{2.3}$$

$$\kappa^{(1)}\frac{\partial C^{(1)}}{\partial n} = \kappa^{(2)}\frac{\partial C^{(2)}}{\partial n} \qquad \text{on } \partial\Omega^{(1)}, \tag{2.4}$$

$$\frac{\partial C^{(2)}}{\partial n} = 0 \qquad \text{on } \partial\Omega^{(2)}, \tag{2.5}$$

where $u_0(x,y)$ is chosen to satisfy the Navier-Stokes equations in $\Omega^{(1)}$, and $C^{(i)}(x,y,z,t)$ is a concentration in $\Omega^{(i)}$, $i = 1,2$. We have the diffusivities $D^{(i)} = \kappa^{(i)}/\rho^{(i)}$, $i = 1,2$, where $\rho^{(1)}$ and $\kappa^{(1)}$ are the density and conductivity of the mobile phase, and $\rho^{(2)}$ and $\kappa^{(2)}$ are the density and conductivity of the stationary phase. The *partition coefficient* K is defined as the ratio of the analyte concentration in the stationary phase to the analyte concentration in the mobile phase. We denote this relationship as $C^{(2)} = KC^{(1)}$, and take K to be constant. This assumption defines *linear* chromatography. Although we do not consider the nonlinear case here, a model of nonlinear chromatography is described in [1]. The linear partition coefficient is discussed in greater detail in Appendix 8. Equation (2.1) describes the advection and diffusion of the concentration in the mobile phase. Equation (2.2) describes unidirectional diffusion in the stationary phase. Equation (2.3) is a consequence of chemical equilibrium between the phases, and (2.4) enforces flux equilibrium. Equation (2.5) indicates that the capillary wall is a zero-flux boundary. For the remainder of this paper, we specialize equations (2.1)-(2.5) to the case of a long narrow column of radius $R(1+\delta)$ with coated walls in a cylindrical coordinate system with radial symmetry, and assume the cross section of the column does not vary with z. The cross-section is shown in Figure 1. The mobile phase $\Omega^{(1)}$ has radius R, and the stationary phase $\Omega^{(2)}$ has a thickness $R\delta > 0$. We choose u_0 to be the velocity profile for Poiseuille flow in a column,

$$u_0(r) = \left\{ \begin{array}{cc} 2U_0\left(1 - \frac{r^2}{R^2}\right) & 0 \le r \le R \\ 0 & r > R \end{array} \right\},$$

where U_0 is the average value of the velocity.

3 Reduced Order Models

In section 3.1, we show that we can solve the two-domain model equations (2.1)-(2.5) by performing a Fourier transform of the concentration in z, then expanding the solution in eigenfunctions. This greatly simplifies the problem and reduces the required computational effort for solution. This procedure can also be applied to the one-domain model equations (1.1)-(1.2). However, in section (3.2), we instead derive Golay's boundary condition (1.2) from the two-domain model. In the process, we show the assumptions under which the one-domain model is valid. In preparation for the investigation of asymmetries in section 4, we first make the one-domain and two-domain eigenvalue problems dimensionless in section 3.3. Finally, in section 3.4, we show how to account for the initial distribution of the concentration within the rescaled models.

3.1 The Eigenvalue Problem for the Two-Domain Model

Let $\widehat{C}^{(i)}(r,\alpha,t)$ be the Fourier transform of the concentration $C^{(i)}(r,z,t)$ with respect to z:

$$\widehat{C}^{(i)}(r,\alpha,t) = \int_{-\infty}^{\infty} e^{-i\alpha z} C^{(i)}(r,z,t)dz \qquad\qquad i = 1,2.$$

Then, $\widehat{C}^{(1)}$, $\widehat{C}^{(2)}$ satisfy

$$\begin{aligned} \frac{\partial \widehat{C}^{(1)}}{\partial t} + i\alpha u_0(r)\widehat{C}^{(1)} &= D^{(1)}\left(\nabla_r^2 \widehat{C}^{(1)} - \alpha^2 \widehat{C}^{(1)}\right) && \text{in } \Omega^{(1)}, \\ \frac{\partial \widehat{C}^{(2)}}{\partial t} &= D^{(2)}\left(\nabla_r^2 \widehat{C}^{(2)} - \alpha^2 \widehat{C}^{(2)}\right) && \text{in } \Omega^{(2)}, \end{aligned}$$

with the boundary conditions

$$\begin{aligned} \widehat{C}^{(2)} &= K\widehat{C}^{(1)} && \text{at } r = R, \\ \kappa^{(1)}\frac{\partial \widehat{C}^{(1)}}{\partial r} &= \kappa^{(2)}\frac{\partial \widehat{C}^{(2)}}{\partial r} && \text{at } r = R, \\ \frac{\partial \widehat{C}^{(2)}}{\partial r} &= 0 && \text{at } r = R(1+\delta), \end{aligned}$$

where $\nabla_r^2 = \frac{\partial^2}{\partial r^2} + \frac{1}{r}\frac{\partial}{\partial r}$ is a Laplacian in the radial direction only.

We can solve the Fourier-transformed equations by expanding the solution in eigenfunctions:

$$\begin{aligned} \widehat{C}^{(1)}(r,\alpha,t) &= \sum_{m=0}^{\infty} a_m \widehat{C}_m^{(1)}(r,\alpha)e^{\lambda_m(\alpha)t}, \\ \widehat{C}^{(2)}(r,\alpha,t) &= \sum_{m=0}^{\infty} a_m \widehat{C}_m^{(2)}(r,\alpha)e^{\lambda_m(\alpha)t}. \end{aligned}$$

The eigenfunctions $\widehat{C}_m^{(1)}(r,\alpha)$, $\widehat{C}_m^{(2)}(r,\alpha)$, and associated eigenvalues $\lambda_m(\alpha)$ must then satisfy the eigenvalue problem

$$\lambda_m \widehat{C}_m^{(1)} + i\alpha u_0(r)\widehat{C}_m^{(1)} = D^{(1)}\left(\nabla_r^2 \widehat{C}_m^{(1)} - \alpha^2 \widehat{C}_m^{(1)}\right) \qquad \text{in } \Omega^{(1)}, \tag{3.1}$$

$$\lambda_m \widehat{C}_m^{(2)} = D^{(2)}\left(\nabla_r^2 \widehat{C}_m^{(2)} - \alpha^2 \widehat{C}_m^{(2)}\right) \qquad \text{in } \Omega^{(2)}, \tag{3.2}$$

with the boundary conditions

$$\widehat{C}_m^{(2)} = K\widehat{C}_m^{(1)} \qquad \text{at } r = R, \tag{3.3}$$

$$\kappa^{(1)}\frac{\partial \widehat{C}_m^{(1)}}{\partial r} = \kappa^{(2)}\frac{\partial \widehat{C}_m^{(2)}}{\partial r} \qquad \text{at } r = R, \tag{3.4}$$

$$\frac{\partial \widehat{C}_m^{(2)}}{\partial r} = 0 \qquad \text{at } r = R(1+\delta), \tag{3.5}$$

for all m.

Computing the solution for all m, α would be very complicated. For the case $\alpha = 0$, we see that our eigenvalue problem is greatly simplified. In particular, if $\delta = 0$, we can see that the resulting problem has eigenvalues

$$\lambda_m(0) = \begin{cases} 0 & m = 0 \\ \frac{D^{(1)}}{R^2}\nu_m & m > 0 \end{cases} \tag{3.6}$$

where $\nu_m \leq 0$ is an eigenvalue of ∇_r^2 with zero Neumann boundary conditions over the unit disk. To determine the concentration at time t we must compute the inverse Fourier transform, which involves the term $e^{\lambda_m(\alpha)t} = e^{(D^{(1)}/R^2)\nu_m t}$. When $D^{(1)}t/R^2 \gg 1$, which holds for t sufficiently large, all of the modes $m > 0$ damp out rapidly in comparison with the $m = 0$ mode. If $\alpha \neq 0$, these modes damp out even faster. This also hold true if $\delta > 0$. Thus, under these assumptions, we need only consider the mode $m = 0$, and solve only for the eigenfunctions $\widehat{C}_0^{(1)}(r,\alpha)$, $\widehat{C}_0^{(2)}(r,\alpha)$, and the eigenvalue $\lambda_0(\alpha)$. Further, we are interested in these terms only for small α. For $m = 0$, equations (3.1)-(3.5) define the simplified two-domain eigenvalue problem.

3.2 Derivation of the One-Domain Model

The equations describing the mobile phase $\Omega^{(1)}$ are identical in both the one-domain and two-domain models. In the stationary phase $\Omega^{(2)}$, an idealized liquid phase coating is extremely thin with respect to the column diameter. Under this assumption, we can greatly simplify the solution of equations (3.1)-(3.5) for the case $m = 0$ by deriving a single "reacting side wall" boundary condition for the mobile phase $\Omega^{(1)}$.

Let us assume that that $\delta \ll 1$. Under this assumption, (3.2) over the domain $\Omega^{(2)}$ can be replaced with

$$D^{(2)}\frac{\partial^2 \widehat{C}_0^{(2)}}{\partial r^2} = \left(\lambda_0 + D^{(2)}\alpha^2\right)\widehat{C}_0^{(2)} \qquad \text{in } \Omega^{(2)}, \tag{3.7}$$

where we have ignored the first derivative term, given that $|\partial^2 \widehat{C}_0^{(2)}/\partial r^2| \gg |\partial \widehat{C}_0^{(2)}/\partial r|$ when $\delta \ll 1$. The first derivative term could have been kept and approximated as $(1/R)(\partial \widehat{C}_0^{(2)}/\partial r)$, although this added complication gives nearly the same result.

Equation (3.7) can be solved explicitly, which means we can create a modified boundary condition for $\widehat{C}_0^{(1)}$ at $r = R$, and then need only solve over the domain $\Omega^{(1)}$. The solution to (3.7) in the domain $\Omega^{(2)}$ is

$$\widehat{C}_0^{(2)}(r) = \left(K\widehat{C}_0^{(1)}(R)\right) \frac{\cosh\left[\left(R\left(1+\delta\right)-r\right)\sqrt{\frac{\lambda_0}{D^{(2)}}+\alpha^2}\,\right]}{\cosh\left[R\delta\sqrt{\frac{\lambda_0}{D^{(2)}}+\alpha^2}\,\right]} \qquad \text{in } \Omega^{(2)},$$

where the boundary conditions (3.3) and (3.5) are satisfied. Taking the derivative and substituting into (3.4) for $m = 0$, the reacting side wall boundary condition takes the form

$$D^{(1)}\frac{\partial \widehat{C}_0^{(1)}}{\partial r} = \quad -D^{(1)}\frac{\kappa^{(2)}}{\kappa^{(1)}}\left(K\widehat{C}_0^{(1)}(R)\right)\sqrt{\frac{\lambda_0}{D^{(2)}}+\alpha^2}\frac{\sinh\left[R\delta\sqrt{\frac{\lambda_0}{D^{(2)}}+\alpha^2}\,\right]}{\cosh\left[R\delta\sqrt{\frac{\lambda_0}{D^{(2)}}+\alpha^2}\,\right]} \qquad \text{at } r = R.$$

We can further simplify the boundary condition by Taylor expanding in δ, and keeping only $O(\delta)$ terms. Our boundary boundary condition takes the form

$$\frac{D^{(1)}}{R}\frac{\partial \widehat{C}_0^{(1)}}{\partial r} = -\frac{k}{2}\widehat{C}_0^{(1)}(R)\left(\lambda_0 + D^{(2)}\alpha^2\right) \qquad \text{at } r = R, \tag{3.8}$$

where we have used the retention factor

$$k = 2K\delta\frac{\kappa^{(2)}}{\kappa^{(1)}}\frac{D^{(1)}}{D^{(2)}}. \tag{3.9}$$

The inverse Fourier transform of (3.8) gives

$$\frac{D^{(1)}}{R}\frac{\partial \widehat{C}^{(1)}}{\partial r} = -\frac{k}{2}\left(\frac{\partial \widehat{C}^{(1)}}{\partial t} + D^{(2)}\frac{\partial^2 \widehat{C}^{(1)}}{\partial z^2}\right) \qquad \text{at } r = R, \tag{3.10}$$

which is the complete boundary condition to $O(\delta)$.

Note that the boundary condition (3.10) agrees with Golay's boundary condition (1.2), except for the $\partial^2 \widehat{C}^{(1)}/\partial z^2$ term. If the α^2 term in (3.8) is neglected, the inverse Fourier transform gives exactly Golay's boundary condition (1.2). Consider (3.8), and recall that $\lambda_0 \sim D^{(1)}/R^2$, from (3.6). We see that the term α^2 can be neglected if $D^{(1)}/D^{(2)} \gg (\alpha R)^2$. As we are interested only in small values of α, $R \ll 1$, and $D^{(1)}/D^{(2)} \approx 10^4$, for typical problem parameters, the α^2 term in (3.8) can safely be neglected, and the boundary condition (1.2) is accurate under these conditions. Our simplified model is

$$\lambda_0 \widehat{C}_0^{(1)} + i\alpha u_0(r)\widehat{C}_0^{(1)} = D^{(1)}\left(\nabla_r^2 \widehat{C}_0^{(1)} - \alpha^2 \widehat{C}_0^{(1)}\right) \qquad \text{in } \Omega^{(1)}, \tag{3.11}$$

$$\frac{D^{(1)}}{R}\frac{\partial \widehat{C}_0^{(1)}}{\partial r} = -\frac{k}{2}\widehat{C}_0^{(1)}(R)\lambda_0 \qquad \text{at } r = R, \tag{3.12}$$

These equations define the one-domain eigenvalue problem, and are in agreement with the equations (1.1)-(1.2).

3.3 Rescaling

We introduce the dimensionless variables

$$\sigma = \frac{R^2}{D^{(1)}}\lambda_0 \qquad \varepsilon = \alpha R \qquad Pe = \frac{U_0 R}{D^{(1)}} \qquad \zeta = \frac{z}{R}$$

$$\xi = \frac{r}{R} \qquad \phi^{(1)} = \frac{\widehat{C}_0^{(1)}}{R} \quad \phi^{(2)} = \frac{\widehat{C}_0^{(2)}}{R} \quad \tau = \frac{D^{(1)}}{R^2}t$$

which give the rescaled two-domain eigenvalue problem

$$\sigma\phi^{(1)} + 2i\varepsilon Pef(\xi)\phi^{(1)} = \frac{\partial^2\phi^{(1)}}{\partial\xi^2} + \frac{1}{\xi}\frac{\partial\phi^{(1)}}{\partial\xi} - \varepsilon^2\phi^{(1)} \qquad \text{in } \widetilde{\Omega}^{(1)}, \tag{3.13}$$

$$\frac{D^{(1)}}{D^{(2)}}\sigma\phi^{(2)} = \frac{\partial^2\phi^{(2)}}{\partial\xi^2} + \frac{1}{\xi}\frac{\partial\phi^{(2)}}{\partial\xi} \qquad \text{in } \widetilde{\Omega}^{(2)}, \tag{3.14}$$

$$\phi^{(2)} = K\phi^{(1)} \qquad \text{at } \xi = 1, \tag{3.15}$$

$$\frac{\partial\phi^{(1)}}{\partial\xi} = \frac{\kappa^{(2)}}{\kappa^{(1)}}\frac{\partial\phi^{(2)}}{\partial\xi} \qquad \text{at } \xi = 1, \tag{3.16}$$

$$\frac{\partial\phi^{(2)}}{\partial\xi} = 0 \qquad \text{at } \xi = 1+\delta, \tag{3.17}$$

where Pe is the Péclet number, $f(\xi) = 1-\xi^2$, $\widetilde{\Omega}^{(1)}$ is the unit disk (the domain $\Omega^{(1)}$ rescaled by a factor R), and $\widetilde{\Omega}^{(2)}$ is an annulus of thickness δ (the domain $\Omega^{(2)}$ rescaled by a factor R). Note that the term $\varepsilon^2\phi^{(2)}$ has been dropped from (3.14) for the same reason that the term involving α^2 was dropped from (3.12).

We realize this is not an ideal scaling for the Péclet number. Other scalings are $U_0L/D^{(1)}$ where L is the column length, or $U_0W/D^{(1)}$, where W is the full width of the concentration distribution at half height. We choose to use the rescaling given above because it produces rescaled equations of the simplest form.

The rescaled simplified one-domain equations (3.11)-(3.12) take the form

$$\sigma\phi^{(1)} + 2i\varepsilon Pef(\xi)\phi^{(1)} = \frac{\partial^2\phi^{(1)}}{\partial\xi^2} + \frac{1}{\xi}\frac{\partial\phi^{(1)}}{\partial\xi} - \varepsilon^2\phi^{(1)} \qquad \text{in } \widetilde{\Omega}^{(1)}, \tag{3.18}$$

$$\frac{\partial\phi}{\partial\xi} = -\frac{k}{2}\phi^{(1)}(1)\sigma \qquad \text{at } \xi = 1. \tag{3.19}$$

3.4 Initial Concentration Distribution

Our models must also account for the shape of the analyte distribution after it enters the column, especially as the initial concentration distribution is in general highly nonsymmetric.

Let $F(r,\alpha)$ represent the unscaled Fourier transform of the initial concentration at time $t = 0$. We may express this function as a linear combination of the eigenmodes in domain $\Omega^{(1)}$:

$$F(r,\alpha) = \sum_{m=0}^{\infty} a_m(\alpha) C_m^{(1)}(r,\alpha).$$

We assume that the initial concentration in the stationary phase $\Omega^{(2)}$ is zero. As we have seen, only the $m = 0$ eigenmode $C_0^{(1)} = \phi^{(1)}$ survives for large τ. We are therefore concerned only with the coefficient $a_0(\varepsilon)$. As our operator in (3.13) is symmetric but not Hermitian, we can isolate $a_0(\alpha)$ by taking the inner product with the corresponding $m = 0$ eigenfunction of the adjoint operator. It can be shown that this eigenfunction of the adjoint operator is just the complex conjugate of $\phi^{(1)}(\xi,\varepsilon)$, which gives

$$a_0(\varepsilon) = \frac{\int_0^1 \xi \phi^{(1)}(\xi,\varepsilon) F(\xi,\varepsilon) d\xi}{\int_0^1 \xi \phi^{(1)}(\xi,\varepsilon)\phi^{(1)}(\xi,\varepsilon) d\xi}$$

where $F(\xi,\varepsilon)$ denotes the dimensionless rescaling of $F(r,\alpha)$, and $a_0(\varepsilon)$ the dimensionless rescaling of $a_0(\alpha)$.

4 Small Wavenumber Expansions: Computing $\sigma(\varepsilon)$

We must apply an inverse Fourier transform to determine our final concentration. We assume that the Fourier-transformed function can be can be replaced with its $m = 0$ eigenmode in the case where $D^{(1)}t/R^2 \gg 1$, as discussed earlier. For this situation, we seek

$$\Phi(\xi,\zeta,\tau) = \frac{1}{2\pi} \int_{-\infty}^{\infty} e^{i\varepsilon\zeta} a_0(\varepsilon) \phi^{(1)}(\xi,\varepsilon) e^{\sigma(\varepsilon)\tau} d\varepsilon, \tag{4.1}$$

The real part of $\sigma(\varepsilon)$ is everywhere nonpositive and has a maximum at $\varepsilon = 0$, meaning that the main contribution of the integral will come for small ε. As such, we consider the expansion of the eigenvalue $\sigma(\varepsilon)$ in the rescaled wavenumbers ε:

$$\sigma(\varepsilon) = \sigma_0 + \sigma_1\varepsilon + \sigma_2\varepsilon^2 + \sigma_3\varepsilon^3 + \dots$$

From (3.6), we see that $\sigma(0) = 0$, which means that $\sigma_0 = 0$.

To discern the physical meaning of σ_1 and σ_2, assume a differential equation of the form $\partial\phi/\partial\tau + f\ \partial\phi/\partial\zeta = D\partial^2\phi/\partial\zeta^2$, take its Fourier transform in ζ, and plug in a solution of assumed form $\exp(\sigma\tau + i\varepsilon\zeta)$. The resulting expression for the eigenvalue is

$$\sigma(\varepsilon) = (-if)\varepsilon + (-D)\varepsilon^2.$$

We see that $\sigma_1 = -if$ describes the effective velocity of the analyte along the column, and $\sigma_2 = -D$ describes the effective diffusion coefficient. Further, we observe that if σ_3 and higher terms are zero, then the concentration will approximate a Gaussian with mean $f\tau$ and variance $\sqrt{2D\tau}$. Thus, for a symmetric initial analyte distribution, there could never

be any asymmetry. his implies σ_3 and higher terms control the asymmetry of the analyte distribution. Of these higher order terms, σ_3 is the leading and dominant term.

We will also compare the computed expressions for σ_1 and σ_2 with the first and second moments determined by Golay [5]. To translate between moments of the distribution and σ_1 and σ_2, observe that $\sigma_1 \equiv -i$(first moment), and that $\sigma_2 \equiv -1/2$(second moment). Golay did not compute third or higher moments. The third term in the expansion, σ_3, is related to the third moment, which is in turn related to the skewness of the distribution. In chromatography, a zero skewness of the concentration distribution would indicate a symmetric distribution, a positive skewness would indicate a "fronting" tail, and a negative skewness a "lagging tail".

In section 4.1, we apply the standard perturbation theory of eigenvalues to the simplified rescaled two-domain equations (3.13)-(3.17) to construct closed-form expressions for σ_1, σ_2, and σ_3. In section 4.2, we perform the same analysis for the corresponding one-domain equations (3.18)-(3.19). We compare with Golay's first and second moments in [5] by performing a series expansion of σ_i, $i = 1, 2, 3$ in δ while holding $D^{(1)}\delta/D^{(2)}$ fixed. We will see that the one-domain equations exactly recover Golay's first and second moments. For the two-domain equations, the first term in the series expansion of σ_1 exactly matches Golay's first moment, and the first term in the series expansion of σ_2 exactly matches Golay's second moment. The subsequent terms in the series expansions provide higher order corrections in δ.

These results are confirmed via numerical experiment in section 7.

4.1 Eigenvalue Perturbation for Two-Domain Model

We are interested in solving the rescaled simplified two-domain equations (3.13)-(3.17) via a perturbation method. We define

$$\sigma(\varepsilon) = \sigma_1\varepsilon + \sigma_2\varepsilon^2 + \sigma_3\varepsilon^3 + \dots \tag{4.2}$$

$$\phi^{(1)}(\xi,\varepsilon) = \phi_0^{(1)}(\xi) + \phi_1^{(1)}(\xi)\varepsilon + \phi_2^{(1)}(\xi)\varepsilon^2 + \phi_3^{(1)}(\xi)\varepsilon^3 + \dots \tag{4.3}$$

$$\phi^{(2)}(\xi,\varepsilon) = \phi_0^{(2)}(\xi) + \phi_1^{(2)}(\xi)\varepsilon + \phi_2^{(2)}(\xi)\varepsilon^2 + \phi_3^{(2)}(\xi)\varepsilon^3 + \dots \tag{4.4}$$

We plug these expansions into (3.13) and (3.14) and collect powers of ε. The $O(1)$ terms give the problem

$$\frac{\partial^2\phi_0^{(1)}}{\partial\xi^2} + \frac{1}{\xi}\frac{\partial\phi_0^{(1)}}{\partial\xi} = 0 \qquad \text{on } \widetilde{\Omega}^{(1)} \tag{4.5}$$

$$\frac{\partial^2\phi_0^{(2)}}{\partial\xi^2} + \frac{1}{\xi}\frac{\partial\phi_0^{(2)}}{\partial\xi} = 0 \qquad \text{on } \widetilde{\Omega}^{(2)}, \tag{4.6}$$

with boundary conditions

$$\phi_0^{(2)} = K\phi_0^{(1)} \qquad \text{at } \xi = 1, \tag{4.7}$$

$$\frac{\partial \phi_0^{(1)}}{\partial \xi} = \frac{\kappa^{(2)}}{\kappa^{(1)}} \frac{\partial \phi_0^{(2)}}{\partial \xi} \qquad \text{at } \xi = 1, \tag{4.8}$$

$$\frac{\partial \phi_0^{(2)}}{\partial \xi} = 0 \qquad \text{at } \xi = 1 + \delta. \tag{4.9}$$

We determine that $\phi_0^{(1)}(\xi) = 1$ by solving (4.5) and requiring that $\phi_0^{(1)}$ be finite at $\xi = 0$. Similarly, we find $\phi_0^{(2)}(\xi) = K$.

Continuing, we find that the $O(\varepsilon)$ terms give

$$\frac{\partial^2 \phi_1^{(1)}}{\partial \xi^2} + \frac{1}{\xi}\frac{\partial \phi_1^{(1)}}{\partial \xi} = \sigma_1 + 2iPef(\xi) \qquad \text{on } \widetilde{\Omega}^{(1)} \tag{4.10}$$

$$\frac{\partial^2 \phi_1^{(2)}}{\partial \xi^2} + \frac{1}{\xi}\frac{\partial \phi_1^{(2)}}{\partial \xi} = \frac{D^{(1)}}{D^{(2)}} K\sigma_1 \qquad \text{on } \widetilde{\Omega}^{(2)}, \tag{4.11}$$

with boundary conditions

$$\phi_1^{(2)} = K\phi_1^{(1)} \qquad \text{at } \xi = 1, \tag{4.12}$$

$$\frac{\partial \phi_1^{(1)}}{\partial \xi} = \frac{\kappa^{(2)}}{\kappa^{(1)}} \frac{\partial \phi_1^{(2)}}{\partial \xi} \qquad \text{at } \xi = 1, \tag{4.13}$$

$$\frac{\partial \phi_1^{(2)}}{\partial \xi} = 0 \qquad \text{at } \xi = 1 + \delta. \tag{4.14}$$

Equations (4.10)-(4.11) have the form

$$\frac{1}{\xi}\frac{\partial}{\partial \xi}\left(\xi \frac{\partial \phi^{(1)}}{\partial \xi}\right) = g^{(1)} \qquad \text{on } \widetilde{\Omega}^{(1)}, \tag{4.15}$$

$$\frac{1}{\xi}\frac{\partial}{\partial \xi}\left(\xi \frac{\partial \phi^{(2)}}{\partial \xi}\right) = g^{(2)} \qquad \text{on } \widetilde{\Omega}^{(2)}. \tag{4.16}$$

along with the boundary conditions (4.12)-(4.14). If we multiply (4.15) by ξ and (4.16) by $\kappa^{(2)}\xi/\kappa^{(1)}$ and integrate, we arrive at

$$\int_0^1 \frac{\partial}{\partial \xi}\left(\xi \frac{\partial \phi^{(1)}}{\partial \xi}\right) d\xi + \frac{\kappa^{(2)}}{\kappa^{(1)}} \int_1^{1+\delta} \frac{\partial}{\partial \xi}\left(\xi \frac{\partial \phi^{(2)}}{\partial \xi}\right) d\xi = \int_0^1 \xi g^{(1)} d\xi + \frac{\kappa^{(2)}}{\kappa^{(1)}} \int_1^{1+\delta} \xi g^{(2)} d\xi. \tag{4.17}$$

We find, after evaluating boundary conditions, that the left hand side of the proceeding equation is zero. This relationship is necessary for the solvability of (4.10)-(4.11) with their boundary conditions, but it can also be shown that this relationship is sufficient. The right hand side of this equation must also be zero, which then defines the *solvability condition*

$$\int_0^1 \xi g^{(1)} d\xi + \frac{\kappa^{(2)}}{\kappa^{(1)}} \int_1^{1+\delta} \xi g^{(2)} d\xi = 0, \tag{4.18}$$

that must hold if we are to determine solutions to the differential equations with their specific boundary conditions.

We apply the solvability condition for the $O(\varepsilon)$ equations (4.10)-(4.11). Solving the resulting equation for σ_1 gives

$$\sigma_1 = \frac{-2iPe\int_0^1 f(\xi)\xi d\xi}{\int_0^1 \xi d\xi + \frac{k}{2}\int_1^{1+\delta}\xi d\xi},$$

where all the terms on the right-hand side are known. The proceeding equation has been simplified in terms of the retention factor k, defined in (3.9).

Solving for σ_1 allows us to solve for $\phi_1^{(1)}$ and $\phi_1^{(2)}$. Knowledge of these terms allows us to again exploit the solvability condition to determine σ_2. We can determine an expression for σ_2 similar in form to the proceeding equation, where all the terms on the right hand side are known and easily evaluated. Once σ_2 is known, we solve for $\phi_2^{(1)}$ and $\phi_2^{(2)}$, and then again exploit the solvability condition to determine σ_3, and so on. This process can be continued indefinitely, although we will stop at σ_3.

After exploiting the solvability condition to determine σ_n, we must then determine $\phi_n^{(1)}$ and $\phi_n^{(2)}$ by solving equations of the form

$$\frac{\partial^2\phi_n^{(1)}}{\partial\xi^2} + \frac{1}{\xi}\frac{\partial\phi_n^{(1)}}{\partial\xi} = \sigma_n + h^{(1)}\left(\sigma_{n-1},\ldots,\sigma_1,\phi_{n-1}^{(1)},\ldots,\phi_0^{(1)}\right) \qquad \text{on } \widetilde{\Omega}^{(1)} \tag{4.19}$$

$$\frac{\partial^2\phi_n^{(2)}}{\partial\xi^2} + \frac{1}{\xi}\frac{\partial\phi_n^{(2)}}{\partial\xi} = \frac{D^{(1)}}{D^{(2)}}K\sigma_n + h^{(2)}\left(\sigma_{n-1},\ldots,\sigma_1,\phi_{n-1}^{(1)},\ldots,\phi_0^{(1)}\right) \qquad \text{on } \widetilde{\Omega}^{(2)}, \tag{4.20}$$

with corresponding boundary conditions

$$\phi_n^{(2)} = K\phi_n^{(1)} \qquad \text{at } \xi = 1, \tag{4.21}$$

$$\frac{\partial\phi_n^{(1)}}{\partial\xi} = \frac{\kappa^{(2)}}{\kappa^{(1)}}\frac{\partial\phi_n^{(2)}}{\partial\xi} \qquad \text{at } \xi = 1, \tag{4.22}$$

$$\frac{\partial\phi_n^{(2)}}{\partial\xi} = 0 \qquad \text{at } \xi = 1+\delta. \tag{4.23}$$

The functions $h^{(1)}$ and $h^{(2)}$ involve only polynomial combinations of ξ^i and $\xi^i\log\xi$, making the differential equations easily solvable at each step. As this process is very systematic, we use *Mathematica* to automate our computations, and determine $\{\sigma_i\}_{i=1}^3$.

Physically realistic values for the ratio of diffusion constants and relative thickness of the stationary phase are $D^{(1)}/D^{(2)} \approx 10^4$ and $\delta \approx 0.002$ [12]. Although $\delta \ll 1$, $(D^{(1)}/D^{(2)})\delta$ is not small. As such, we hold $(D^{(1)}/D^{(2)})\delta$ constant and perform a series expansion of σ_1,

σ_2, and σ_3 in δ. Upon simplification, we arrive at the following expansions for $\{\sigma_i\}_{i=1}^3$:

$$\sigma_1 = -\left(\frac{iPe}{1+k}\right) + \left(\frac{iPe}{2}\frac{k}{(1+k)^2}\right)\delta + \ldots, \tag{4.24}$$

$$\sigma_2 = \frac{-1}{1+k}\left(1 + \frac{11k^2+6k+1}{48\,(1+k)^2}Pe^2\right) - \frac{k}{2(1+k)^2}\left(-1 + \frac{-11k^2+10k+3}{48\,(1+k)^2}Pe^2\right)\delta \tag{4.25}$$
$$- \left(\frac{kPe^2}{16(1+k)^3}\right)\frac{D^{(1)}}{D^{(2)}}\delta^2 + \ldots,$$

$$\sigma_3 = \frac{iPe}{12(1+k)^3}\left(k(1+4k) + \frac{177k^4+122k^3+44k^2+10k+1}{240\,(1+k)^2}Pe^2\right) \tag{4.26}$$
$$+ \frac{ikPe}{24(1+k)^4}\left((1+6k-4k^2) + \frac{-177k^4+464k^3+234k^2+48k+5}{240(1+k)^2}Pe^2\right)\delta$$
$$+ \frac{ikPe}{3(1+k)^3}\left(2 - \frac{1+2k-11k^2}{24(1+k)^2}Pe^2\right)\frac{D^{(1)}}{D^{(2)}}\delta^2 + \ldots.$$

Note that σ_1 and σ_3 are purely imaginary, while σ_2 is purely real. These expansions can be continued, and only the first two terms of each expansion are given here. Since Pe, k, $D^{(1)}$, $D^{(2)}$ are always positive, and $0 < \delta < 1$, we see that the signs of σ_1 and σ_2 are always negative, which ensures that the concentration peak always moves with the flow of the carrier gas, and that diffusion always leads to broader bands on the column. Additionally, note that σ_3 goes to zero as k approaches ∞.

Further, observe that the sign of σ_3 is constrained to be nonnegative. The sign of σ_3, which is the same as the sign of the third moment of the distribution of the concentration, indicates whether the asymmetry is "fronting" or "tailing". In statistics, the sign of the third moment of a distribution determines whether the asymmetry is "left-skewed" or "right-skewed", in the same manner. For chromatography, we see by analogy that if σ_3 is negative, a "tailing" peak is predicted, and if σ_3 is positive, a "fronting" peak is predicted. This means that the the equations for linear chromatography in a homogeneous column can *never* lead to "tailing" peaks. This theory predicts that only "fronting" peaks are possible, and strongly suggests that a nonlinear chromatography model is necessary to explain tailing peaks.

In comparing with the predictions of Golay, we note that his first moment agrees with the first term in (4.24), and that his second moment (equation (30) in [5]) agrees with the first term in (4.25).

In the next section, we will compare with the corresponding expansions for the one-domain model, and see that the one-domain equations recover only the first term in the above series expansions. Note that (4.24)-(4.26) are valid up to $O(\delta)$, whereas the results in the next section are valid only to $O(1)$.

4.2 Eigenvalue Perturbation for One-Domain Model

We are interested in solving the one-domain chromatography equations (3.18)-(3.19) via a perturbation method. We define

$$\sigma(\varepsilon) = \sigma_0 + \sigma_1\varepsilon + \sigma_2\varepsilon^2 + \sigma_3\varepsilon^3 + \dots \tag{4.27}$$

$$\phi(\xi,\varepsilon) = \phi_0(\xi) + \phi_1(\xi)\varepsilon + \phi_2(\xi)\varepsilon^2 + \phi_3(\xi)\varepsilon^3 + \dots \tag{4.28}$$

where we have set $\phi \equiv \phi^{(1)}$, as we only consider the single domain $\widetilde{\Omega}^{(1)}$ here. Note that the eigenvalue $\sigma(\varepsilon)$ in this section is distinct from the eigenvalue in the last section, because we are considering the one-domain equations here.

Plugging the proceeding expansions into (3.18) and collecting powers of ε gives $\phi_0 = 1$, to $O(1)$, where we again have $\sigma_0 = 0$. Continuing, we find that the $O(\varepsilon)$ expansion gives

$$\frac{\partial^2\phi_1}{\partial\xi^2} + \frac{1}{\xi}\frac{\partial\phi_1}{\partial\xi} = \sigma_1 + 2iPef(\xi) \qquad \text{on } \widetilde{\Omega}^{(1)} \tag{4.29}$$

$$\frac{\partial\phi_1}{\partial\xi} = -\frac{k}{2}\sigma_1 \qquad \text{at } \xi = 1. \tag{4.30}$$

The proceeding equations have the form

$$\frac{1}{\xi}\frac{\partial}{\partial\xi}\left(\xi\frac{\partial\phi}{\partial\xi}\right) = g^{(1)} \qquad \text{on } \widetilde{\Omega}^{(1)}, \tag{4.31}$$

$$\frac{\partial\phi}{\partial\xi} = g^{(2)} \qquad \text{at } \xi = 1. \tag{4.32}$$

If we multiply (4.31) by ξ and integrate, we arrive at

$$\int_0^1 \frac{\partial}{\partial\xi}\left(\xi\frac{\partial\phi}{\partial\xi}\right)d\xi = \int_0^1 g^{(1)}\xi d\xi \tag{4.33}$$

We find, after evaluating boundary conditions, that the left hand side of the proceeding equation is $g^{(2)}$. This relationship is necessary for the solvability of (4.29) with its boundary conditions, but one can also show that this argument is sufficient. Setting the right-hand side equal to $g^{(2)}$ serves to define the *solvability condition*

$$\int_0^1 g^{(1)}\xi d\xi = g^{(2)}, \tag{4.34}$$

which must hold if we are to determine solutions to the differential equations, given their specific boundary conditions.

We may proceed in the same systematic fashion as in the previous section, using the compatibility condition to determine the next term in the series expansion of σ, and then solving the differential equation of that order to determine the next term in the series expansion of ϕ. We apply the solvability condition for the $O(\varepsilon)$ equations. Solving the resulting equation for σ_1 gives

$$\sigma_1 = \frac{-iPe\int_0^1 f(\xi)\xi d\xi}{\int_0^1 \xi d\xi + \frac{k}{2}}, \tag{4.35}$$

an expression we can easily compute because all terms on the right-hand side are known and easily evaluated.

Solving for σ_1 allows us to solve for ϕ_1. Knowledge of this function allows us to again exploit the solvability condition to determine σ_2. We can determine an expression for σ_2 similar in form to the proceeding equation, where all the terms on the right hand side are known and easily evaluated. Once σ_2 is known, we solve for ϕ_2, and then again exploit the solvability condition to determine σ_3, and so on. This process can be continued indefinitely, although we will stop at σ_3.

After exploiting the solvability condition to determine σ_n, we must then determine ϕ_n by solving equations of the form

$$\frac{\partial^2 \phi_n}{\partial \xi^2} + \frac{1}{\xi}\frac{\partial \phi_n}{\partial \xi} = \sigma_n + h^{(1)}\left(\sigma_{n-1}, \ldots, \sigma_1, \phi_{n-1}, \ldots, \phi_0\right) \qquad \text{on } \widetilde{\Omega}^{(1)} \tag{4.36}$$

with corresponding boundary condition

$$\frac{\partial \phi_n}{\partial \xi} = -\frac{k}{2}\sigma_n + h^{(2)}\left(\sigma_{n-1}, \ldots, \sigma_1, \phi_{n-1}, \ldots, \phi_0\right) \qquad \text{on } \widetilde{\Omega}^{(2)}, \tag{4.37}$$

The functions $g^{(1)}$ and $g^{(2)}$ involve only polynomial combinations of known quantities, making the differential equations easily solvable at each step. Automating the process with *Mathematica*, we compute $\{\sigma_i\}_{i=1}^{3}$. The *exact* results for the one-domain model are shown below. Note that they agree precisely with the first term in each series (4.24)-(4.26).

$$\sigma_1 = -\left(\frac{iPe}{1+k}\right), \tag{4.38}$$

$$\sigma_2 = \frac{-1}{1+k}\left(1 + \frac{11k^2+6k+1}{48\left(1+k\right)^2}Pe^2\right), \tag{4.39}$$

$$\sigma_3 = \frac{iPe}{12(1+k)^3}\left(k(1+4k) + \frac{177k^4+122k^3+44k^2+10k+1}{240\left(1+k\right)^2}Pe^2\right) \tag{4.40}$$

We emphasize that these results are valid only when $\delta \ll 1$. For larger δ, the expansions in (4.24)-(4.26) are required. Again, we observe that the signs of σ_1 and σ_2 are always negative, and that the sign of σ_3 is never negative, meaning that only fronting peaks, not tailing peaks, are predicted by this model. Finally, we note that (4.38) and (4.39) agree exactly with Golay's results in [5]. Had Golay used his model to predict asymmetries, he would have arrived at (4.40).

5 Return to Normality

Here, we examine sources for asymmetry in the concentration distribution, and provide an estimate of the time required for a return to normality. For the case of Taylor dispersion with non-reacting side walls, this problem was previously considered by Chatwin [3]. We will see that for linear chromatography in a homogeneous column, asymmetries damp out relatively quickly. For ease of notation, we first define $\sigma_1 = -i\mu_1$, $\sigma_2 = -\mu_2$, and $\sigma_3 = i\mu_3$,

where $\mu_1, \mu_2, \mu_3 \in \mathbb{R}^+$. We are interested in approximating

$$\Phi(r, \zeta, \tau) \approx \frac{1}{2\pi} \int_{-\infty}^{\infty} a_0(\varepsilon)\phi^{(1)}(\xi, \varepsilon)e^{i\varepsilon\zeta}e^{\left(-i\mu_1\varepsilon - \mu_2\varepsilon^2 + i\mu_3\varepsilon^3\right)\tau} d\varepsilon.$$

In the model we consider, asymmetry can be caused by three sources. We will consider each in isolation. In section 5.1 we consider the effects of σ_3. We will see that this term is the dominant source of asymmetries. This term contributes only to asymmetries when nonzero, and then only produces fronting peaks. In section 5.2 we consider the effects of the initial concentration distribution, represented by $a_0(\varepsilon)$, and in section 5.3 we consider the effects of the eigenfunction $\phi^{(1)}(\xi, \varepsilon)$. These last two sources of asymmetries can be neglected with respect to the contributions from σ_3, but we compute them for completeness.

5.1 Effects of the term σ_3

Although σ_3 may introduce an asymmetry, the concentration will eventually return to a normal distribution, given sufficient time. Here, we provide an estimate of the time required for a return to normality by approximating the inverse Fourier transform through neglecting the terms σ_4 and higher. Here, we assume the first-order approximations $a_0(\varepsilon) = 1$ and $\phi^{(1)}(\xi, \varepsilon) = 1$, so that we may consider the effects of σ_3 in isolation. We consider the inverse Fourier transform

$$\frac{1}{2\pi} \int_{-\infty}^{\infty} e^{i\varepsilon\zeta}e^{\left(-i\mu_1\varepsilon - \mu_2\varepsilon^2 + i\mu_3\varepsilon^3\right)\tau} d\varepsilon,$$

where we have defined

$$\zeta_0 \equiv \frac{\zeta - \mu_1\tau}{\sqrt{\tau}}.$$

Let $s^2 = \tau\varepsilon^2$. We may reexpress the integrand in terms of s as

$$e^{-\mu_2 s^2 + i\zeta_0 s}e^{i\mu_3\left(s^3/\sqrt{\tau}\right)}.$$

We are interested in $\tau \gg 1$, and thus write a series expansion for the rightmost term, giving

$$e^{i\mu_3\left(s^3/\sqrt{\tau}\right)} \approx 1 + i\mu_3\frac{s^3}{\sqrt{\tau}}.$$

Evaluating the resulting integral gives

$$\left(\frac{1}{\sqrt{\tau}}\right)\frac{1}{2\sqrt{\pi\mu_2}}e^{-\zeta_0^2/(4\mu_2)} + \left(\frac{\mu_3\zeta_0(\zeta_0^2 - 6\mu_2)}{8\mu_2^3\tau}\right)\frac{1}{2\sqrt{\pi\mu_2}}e^{-\zeta_0^2/(4\mu_2)}.$$

The first term on the right-hand side is a gaussian with mean $\mu_1\tau$ and variance $\sqrt{2\mu_2\tau}$; the term we would expect if μ_3 were zero. The coefficient of the second term is the nonsymmetric contribution. We see that it goes to zero $1/\sqrt{\tau}$ faster than the symmetric leading term.

In particular, this means asymmetries due to σ_3 will go to zero as time progresses, and the rate in which they go to zero varies with μ_3/μ_2^3. This means that a larger diffusion rate μ_2 corresponds to a faster return to normality. Additionally, a smaller μ_3 also corresponds to a faster return to normality. How the problem parameters control the magnitude of σ_3 was discussed in sections 4.1 and 4.2, where it was shown that linear chromatography predicts only fronting peaks, and never tailing peaks.

5.2 Effects of the Initial Concentration: $a_0(\varepsilon)$

The initial distribution of the concentration, represented through the function $a_0(\varepsilon)$, is generally the source of an asymmetry, although this asymmetry will damp out over time. We begin by approximating $a_0(\varepsilon)$ as $a_0(\varepsilon) \approx \beta_0 + i\beta_1\varepsilon$.

Here, we assume the first-order approximation $\phi^{(1)}(\varepsilon) = 1$ and that σ_3 and higher terms are zero, so that we may consider the effects of $a_0(\varepsilon)$ in isolation. We consider the inverse Fourier transform

$$\frac{1}{2\pi}\int_{-\infty}^{\infty} e^{i\varepsilon\zeta}\left(\beta_0 + i\beta_1\varepsilon\right) e^{\left(-i\mu_1\varepsilon-\mu_2\varepsilon^2\right)\tau} d\varepsilon.$$

Evaluating the integral gives

$$\left(\frac{\beta_0}{\sqrt{\tau}}\right)\frac{1}{2\sqrt{\pi\mu_2}}e^{-\zeta_0^2/(4\mu_2)} + \left(\frac{\beta_1\zeta_0}{2\mu_2\tau}\right)\frac{1}{2\sqrt{\pi\mu_2}}e^{-\zeta_0^2/(4\mu_2)}. \tag{5.1}$$

The first term is a gaussian with mean $\mu_1\tau$ and variance $\sqrt{2\mu_2\tau}$; the term we would expect if β_1 were zero. In particular, this would be the case if the initial concentration took the form of the eigenmode $\phi^{(1)}$. For $|\beta_1/\beta_0| \ll 1$, β_1 does not introduce an asymmetry and instead corresponds to a shifted gaussian, which we now show.

Consider the gaussian function

$$g(x) = \left(\frac{\beta_0}{\sqrt{\tau}}\right)\frac{1}{2\sqrt{\pi\mu_2}}e^{-(x-\frac{\beta_1}{\beta_0}\frac{1}{\sqrt{\tau}})^2/(4\mu_2)},$$

and the first-order Taylor series expansion of $g(x)$ about the point $\zeta_0 - \frac{\beta_1}{\beta_0}\frac{1}{\sqrt{\tau}}$:

$$g(x) \approx \left(\frac{\beta_0}{\sqrt{\tau}}\right)\frac{1}{2\sqrt{\pi\mu_2}}e^{-\zeta_0^2/(4\mu_2)} - \left(\frac{\beta_0\zeta_0}{2\mu_2\tau}\right)\frac{1}{2\sqrt{\pi\mu_2}}e^{-\zeta_0^2/(4\mu_2)}\left(x - \zeta_0 - \frac{\beta_1}{\beta_0}\frac{1}{\sqrt{\tau}}\right).$$

Evaluating this expansion at the point $x = \zeta_0$ gives

$$g(\zeta_0) \approx \left(\frac{\beta_0}{\sqrt{\tau}}\right)\frac{1}{2\sqrt{\pi\mu_2}}e^{-\zeta_0^2/(4\mu_2)} + \left(\frac{\beta_1\zeta_0}{2\mu_2\tau}\right)\frac{1}{2\sqrt{\pi\mu_2}}e^{-\zeta_0^2/(4\mu_2)},$$

which is precisely (5.1). Thus, (5.1) is approximately equal to

$$g(\zeta_0) = \left(\frac{\beta_0}{\sqrt{\tau}}\right)\frac{1}{2\sqrt{\pi\mu_2}}e^{-(\zeta_0-\frac{\beta_1}{\beta_0}\frac{1}{\sqrt{\tau}})^2/(4\mu_2)},$$

which, being a shifted gaussian, is still a symmetric function. One can also view this result as a change in the frame of reference. It is always possible to select a frame of reference such that α_1 is zero, and thus it cannot be the source of asymmetric peaks.

To analyze the rate at which an asymmetry in the initial concentration is diminished, we must instead consider a higher-order wavenumber expansion of $a_0(\varepsilon)$. We let $a_0(\varepsilon) \approx \beta_0 + i\beta_1\varepsilon + \beta_2\varepsilon^2$. The contribution from the β_2 term is

$$\frac{\beta_2}{2\pi}\int_{-\infty}^{\infty}\varepsilon^2 e^{i\zeta_0\sqrt{\tau}\varepsilon-\mu_2\tau\varepsilon^2}d\varepsilon = \left(\frac{\beta_2(2\mu_2-\zeta_0^2)}{4\mu_2^2\tau\sqrt{\tau}}\right)\frac{1}{2\sqrt{\pi\mu_2}}e^{-\zeta_0^2/(4\mu_2)}.$$

The leading coefficient varies with $\beta_2/(2\mu_2\tau)$, and goes to zero $1/\tau$ faster than the symmetric leading term in (5.1). In particular, this means asymmetries due to the initial concentration distribution go to zero as time progresses, and the rate in which they go to zero varies with $1/\mu_2$, the term governing the diffusion rate. A greater rate of diffusion means that asymmetries of the initial concentration will damp out at a correspondingly greater rate, as we would expect. Further, recall that the nonsymmetric contribution of σ_3 went to zero $1/\sqrt{\tau}$ faster than the leading symmetric term, meaning that the nonsymmetric contribution of the initial concentration can be neglected when compared to the nonsymmetric contribution of σ_3, for long times.

5.3 Effects of the Eigenfuncton: $\phi_1^{(1)}$

The eigenfunction $\phi_1^{(1)}$ can also introduce an asymmetry, although this asymmetry will also damp out over time. In this section, we will approximate the eigenfunction as $\phi^{(1)}(\xi,\varepsilon) \approx \phi_0^{(1)}(\xi) + \phi_1^{(1)}(\xi)\varepsilon + \phi_2^{(1)}(\xi)\varepsilon^2 = 1 + ip_1^{(1)}(\xi)\varepsilon + p_2^{(1)}(\xi)\varepsilon$, where $p_1^{(1)}(\xi)$ and $p_2^{(1)}(\xi)$ are real-valued functions. From the series expansions in section 4, we know that $\phi_0^{(1)} = 1$, $\phi_1^{(1)}$ is purely imaginary, and $\phi_2^{(1)}$ is purely real. From the previous section, we know that so long as $|p_1^{(1)}(\xi)| \ll 1$, the term $p_1^{(1)}(\xi)$ acts to produce a shifted gaussian and does not introduce an asymmetry. We thus consider the contribution of the term $p_2^{(1)}(\xi)$.

We assume the first-order approximation $a_0(\varepsilon) = 1$ and that σ_3 and higher terms are zero, so that we may consider the effects of $\phi^{(1)}$ in isolation. In analogy with the previous section, we consider the inverse Fourier transform

$$\frac{p_2^{(1)}(\xi)}{2\pi}\int_{-\infty}^{\infty}\varepsilon^2 e^{i\zeta_0\sqrt{\tau}\varepsilon-\mu_2\tau\varepsilon^2}d\varepsilon = \left(\frac{p_2^{(1)}(\xi)(2\mu_2-\zeta_0^2)}{4\mu_2^2\tau\sqrt{\tau}}\right)\frac{1}{2\sqrt{\pi\mu_2}}e^{-\zeta_0^2/(4\mu_2)}.$$

The leading coefficient varies with $p_2^{(1)}(\xi)/(4\mu_2\tau)$, and goes to zero $1/\tau$ faster than the symmetric leading term. Again recall that the nonsymmetric contribution of σ_3 went to zero $1/\sqrt{\tau}$ faster than the leading symmetric term, meaning that the nonsymmetric contribution of the eigenfunction can be neglected when compared to the nonsymmetric contribution of σ_3, for long times.

6 Minimum Height Equivalent to a Theoretical Plate

In general, it is desirable to choose an average carrier gas velocity that minimizes the theoretical plate height. We will consider the one-domain model, and utilize the equations (4.38)-(4.40). The (dimensionless) rate of diffusion is $-2\sigma_2$. The (dimensionless) time τ required for an analyte to traverse a column of (dimensionless) length L/R while travelling at a (dimensionless) speed $i\sigma_1$ is $\tau = (L/R)/(i\sigma_1)$. We thus seek to minimize the total diffusion

$$-2\sigma_2\tau = -\frac{2L}{iR}\frac{\sigma_2}{\sigma_1} = \left(\frac{2}{Pe} + \frac{11k^2+6k+1}{24(1+k)^2}Pe\right)\frac{L}{R}.$$

We note that the proceeding equation can be considered a rescaling of the height equivalent to a theoretical plate (HETP) for the column. A plot of the HETP vs. Pe is commonly called a *Golay plot*. Setting the derivative of this equation with respect to Pe equal to zero and solving for the optimal Péclet number Pe^{opt} gives

$$Pe^{opt} = 4\sqrt{3}\frac{1+k}{\sqrt{1+6k+11k^2}}.$$

Plugging this into the expression for the HETP gives the (dimensionless) minimum theoretical plate height. Multiplying the result by R gives

$$\frac{\sqrt{1+6k+11k^2}}{\sqrt{3}(1+k)}L,$$

the unscaled result, in agreement with [5].

7 Numerical Results

In this section we confirm our asymptotic analysis through numerical experiment. Equations (3.13)-(3.17) describe a two-point boundary value problem, and can be solved with the shooting method [4]. This allows numerical determination of $\sigma(\varepsilon)$ and $\phi(\xi,\varepsilon)$ for small ε. This data can be fit with a relatively low-order polynomial, and that polynomial can be used compute the inverse Fourier transform and determine the concentration for all times τ. In this section, assume the initial concentration is strongly oriented with $\phi^{(1)}$ and compute the inverse Fourier transform

$$\frac{1}{2\pi}\int_{-\infty}^{\infty}\widehat{\phi}^{(1)}(\varepsilon)e^{i\varepsilon\zeta}e^{\sigma(\varepsilon)\tau}d\varepsilon, \tag{7.1}$$

where

$$\widehat{\phi}^{(1)}(\varepsilon) \equiv 2\int_0^1 \xi\phi^{(1)}(\xi,\varepsilon)d\xi \tag{7.2}$$

is the average of $\phi^{(1)}$ over a cross-section.

We use this process to solve the two-domain eigenproblem numerically for a given set of problem parameters. We then compare these results with the asymptotic expansions computed in section 4, and with the predictions of Golay.

Consider the two-phase model with the following problem parameters: [12]

$$R = 0.125 \text{ mm} \qquad L = 30 \text{ m} \qquad U_0 = 0.17 \text{ m / s}$$

$$D^{(1)} = 0.4 \text{ cm}^2/\text{s} \qquad \kappa^{(1)} = 6.56\times10^{-5}\tfrac{\text{g}}{\text{cm}\cdot\text{s}} \qquad K = 0.0854$$

$$D^{(2)} = 6\times10^{-6} \text{ cm}^2/\text{s} \qquad \kappa^{(2)} = 5.76\times10^{-6}\tfrac{\text{g}}{\text{cm}\cdot\text{s}} \qquad \delta = 0.002$$

where L is the length of the column. From (3.9), we have $k = 2$. Note that $D^{(1)}\tau/R^2 \gg 1$ for any reasonable $\tau > 0$, so we are justified in considering only the $m = 0$ eigenmode. For the rescaled models, we have the dimensionless parameters

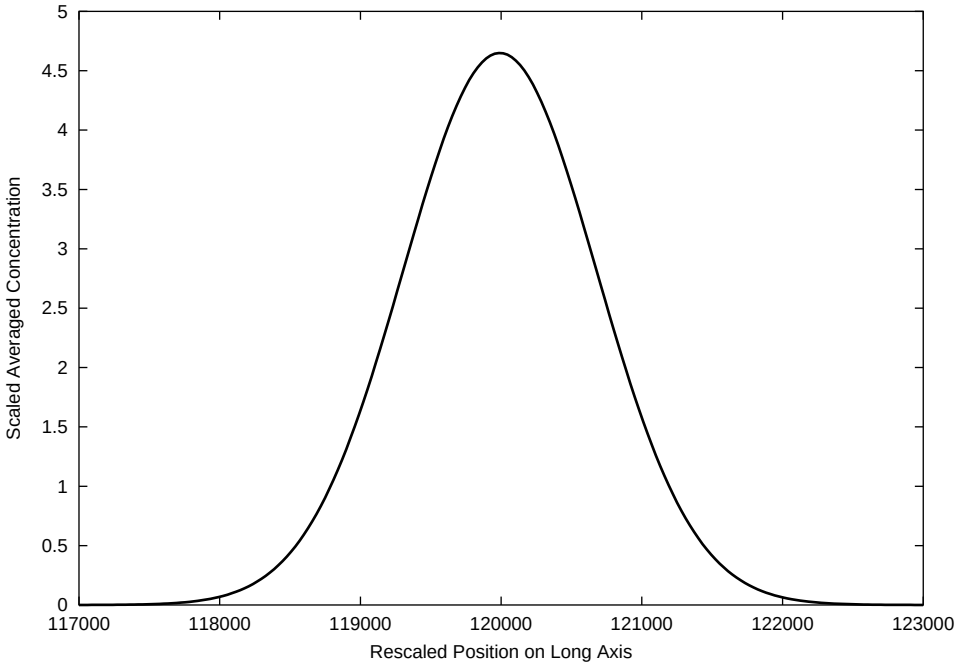

Figure 3. Scaled averaged value of analyte concentration plotted along long axis of column at time $\tau = 6.78 \times 10^5$, approximately halfway along the length of the column. In this example, the curve is symmetric.

$$\frac{D^{(1)}}{D^{(2)}} = 6.6667 \times 10^4 \quad Pe = 0.5313 \quad \delta = 0.002$$

$$\frac{\kappa^{(1)}}{\kappa^{(2)}} = 11.388 \qquad\qquad K = 0.0854$$

A numerical solution of the two-domain eigenvalue problem (3.13)-(3.17) by the means discussed in this section produces, after application of the inverse Fourier transform (7.1), the image shown in Figure 3. This curve is symmetric about the peak. Predictions of the one-domain and two-domain models are tabulated in Table 1, as well as Golay's predictions, and the results from numerical solution of (3.13)-(3.17). Note that all models agree reasonably well.

8 Conclusions

We developed from first principles a general model for linear chromatography in a tubular column. We used this model to develop closed-form expressions for the terms σ_1, σ_2, and σ_3 which control the concentration velocity, diffusion, and asymmetry, respectively. We showed analytically that the phenomenon known as "tailing" can never occur under a homogeneous linear chromatography model. For situations where asymmetries arise ("fronting" peaks)

Table 1. Predictions of the one-domain and two-domain models, along with results from a numerical polynomial curve fit. There is excellent agreement between the asymptotic prediction and numerical result.

	Polynomial Fit	Two-Domain Model	One-Domain Model	Golay Predicted
σ_0	4.00020×10^{-11}	0.00000×10^{0}	0.00000×10^{0}	0.00000×10^{0}
σ_1	$-1.76979\times10^{-1}\ i$	$-1.76979\times10^{-1}\ i$	$-1.77097\times10^{-1}\ i$	$-1.77097\times10^{-1}\ i$
σ_2	-3.47405×10^{-1}	-3.47405×10^{-1}	-3.45771×10^{-1}	-3.45771×10^{-1}
σ_3	$3.75483\times10^{-2}\ i$	$3.75483\times10^{-2}\ i$	$3.03723\times10^{-2}\ i$	N/A

we analyze the rate at which the concentration distribution returns to a normal distribution. We then confirmed our analysis through numerical experiment.

References

[1] A. Ladurelli A. Jaulmes, C. Vidal-Madjar and G. Guiochon. Study of peak profiles in nonlinear gas chromatography. 1. Derivation of a theoretical model. *J. Phys. Chem.*, 88:5379–5385, 1984.

[2] R. Aris. On the dispersion of a solute in a fluid flowing through a tube. *Proceedings of the Royal Society of London. Series A, Mathematical and Physical Sciences*, 235(1200):67–77, September 1956.

[3] P. C. Chatwin. The approach to normality of the concentration of a solute in a solvent flowing along a straight pipe. *J. Fluid Mech.*, 43(2):321–352, 1970.

[4] Walter Gautschi. *Numerical Analysis: An Introduction.* Birkhäuser Verlag, Basel, Switzerland, 1997.

[5] Marcel J. E. Golay. Theory of chromatography in open and coated tubular columns with round and rectangular cross-sections. In D. H. Desty, editor, *Gas Chromatography 1958*, pages 36–53. Butterworths Publications LTD., 1958.

[6] David W. Grant. *Capillary Gas Chromatography.* Separation Science Series. John Wiley & Sons, 1996.

[7] Robert Lee Grob and Eugene F. Barry, editors. *Modern practice of gas chromatography.* Wiley-Interscience, 4$^{\text{th}}$ edition, 2004.

[8] Richard J. Laub and Robert L. Pecsok, editors. *Physicochemical Applications of Gas Chromatography.* Wiley-Interscience, 1978.

[9] Kanji Miyabe and Georges Guiochon. Peak tailing and column radial heterogeneity in linear chromatography. *J. Chromatogr. A*, 830:263–274, 1999.

[10] Geoffrey Taylor. Dispersion of soluble matter in solvent flowing slowly through a tube. *Proceedings of the Royal Society of London. Series A, Mathematical and Physical Sciences*, 219(1137):186–203, August 1953.

[11] Geoffrey Taylor. Conditions under which dispersion of a solute in a stream of solvent can be used to measure molecular diffusion. *Proceedings of the Royal Society of London. Series A, Mathematical and Physical Sciences*, 225(1163):473–477, September 1954.

[12] Joshua Whiting, April 2005. Sandia National Laboratories, personal communication.

APPENDIX

Derivation of Partition Coefficient *K*

At equilibrium, the solute chemical potential $\mu^{(1)}$ in the mobile phase is equal to the chemical potential $\mu^{(2)}$ in the stationary phase:

$$\mu^{(1)} = \mu^{(2)},$$

where

$$\mu^{(i)} = \mu_0^{(i)} + R_u T \ln a^{(i)}, \qquad i = 1, 2,$$

where R_u is the universal gas constant, and T is the absolute temperature. The solute activity in the i^{th} phase is denoted by $a^{(i)}$, and $\mu_0^{(i)}$ is the solute chemical potential at some unit activity. Replacing the activity $a^{(i)}$ by the concentration $C^{(i)}$, we have

$$\mu_0^{(1)} + R_u T \ln C^{(1)} = \mu_0^{(2)} + R_u T \ln C^{(2)}.$$

The ratio of the two concentrations is then given as [8]

$$K \equiv \frac{C^{(2)}}{C^{(1)}} = \exp\left(\frac{\mu_0^{(1)} - \mu_0^{(2)}}{R_u T}\right).$$

It is assumed that $\mu_0^{(1)} - \mu_0^{(2)}$ is a constant, so that α is invariant in the system. Note this this requires the temperature T to be held constant.

DISTRIBUTION:

1 MS 0370
Timothy Trucano, 1411

1 MS 0892
Dan Trudell, 1764

1 MS 0892
Joe Simonson, 1764

3 MS 1425
Joshua Whiting, 1764

3 MS 1110
Michael Parks, 1414

3 MS 1110
Louis Romero, 1414

1 MS 1110
Pavel Bochev, 1414

1 MS 1110
David Day, 1414

1 MS 1110
Scott Collis, 1414

1 MS 1110
David Womble, 1410

3 MS 9018
Central Technical Files, 8945-1

2 MS 0899
Technical Library, 9616